



Published in final edited form as:

*J Mater Sci Mater Med.* 2012 August ; 23(8): 2037–2046. doi:10.1007/s10856-012-4652-0.

## Polymer-coated cannulas for the reduction of backflow during intraparenchymal infusions

**Louis C. Vazquez,**

Department of Chemical Engineering, University of Florida, Gainesville, FL 32611, USA

**Erik Hagel,**

Department of Mechanical and Aerospace Engineering, University of Florida, 212 MAE-A, Gainesville, FL 32611, USA

**Bradley J. Willenberg,**

Department of Material Science and Engineering, University of Florida, Gainesville, FL 32611, USA

**Wei Dai,**

Department of Mechanical and Aerospace Engineering, University of Florida, 212 MAE-A, Gainesville, FL 32611, USA

**Fernando Casanova,**

Department of Mechanical and Aerospace Engineering, University of Florida, 212 MAE-A, Gainesville, FL 32611, USA

**Christopher D. Batich,** and

Department of Material Science and Engineering, University of Florida, Gainesville, FL 32611, USA

**Malisa Sarntinoranont**

Department of Mechanical and Aerospace Engineering, University of Florida, 212 MAE-A, Gainesville, FL 32611, USA

Malisa Sarntinoranont: msarnt@ufl.edu

### Abstract

Infusate backflow or leak-back along the cannula track can occur during intraparenchymal infusions resulting in non-specific targeting of therapeutic agents. The occurrence of backflow depends on several variables including cannula radius, infusate flow rate, and tip location. In this study, polymer coatings that swell in situ were developed and tested with in vitro hydrogel experiments for backflow reduction. Coatings were applied to the external cannula surface in a dual layer arrangement with a poly(vinyl alcohol) outer layer atop an inner poly(ethylene oxide) and alginate layer. Once these coated cannulas were inserted and allotted an 8–10 min waiting period for hydration, backflow during infusions of 4.0  $\mu\text{l}$  of a macromolecular tracer (Evans Blue labeled albumin) was reduced significantly under flow rates of 0.3–0.6  $\mu\text{l}/\text{min}$ , allowing for more effective distribution within targeted regions. Polymer coating thicknesses before and after hydrations were 0.035 and 0.370 mm, respectively. Also, backflow data was fit to a model to estimate the effective local compressive stress caused by the hydrated polymers. After withdrawal of the cannula from the insertion site, the hydrated polymer coatings remained within the cavity left in the hydrogel tissue phantom and formed a seal at the infusion site that prevented further

backflow during needle withdrawal. Ex vivo infusions in excised porcine brain tissues also showed significant backflow reduction while also demonstrating the ability to leave a polymer seal in the tissue cavity after cannula removal. Thus, application of these polymers as needle or cannula coatings offers a potentially simple method to improve targeting for local drug delivery.

## 1 Introduction

Local drug delivery via intraparenchymal infusions in which infusate is infused directly into tissue (e.g., convection-enhanced delivery) has gained increased consideration for the treatment of several neoplastic, epileptic, and neurodegenerative disorders [1–4]. The advantages of intraparenchymal infusions derive from their potential to directly distribute high concentrations of therapeutic agents of various sizes over large tissue volumes and bypass transport barriers such as the blood brain barrier. However, a limitation of these infusions is backflow or leak-back of infusate up the outer cannula track that occurs due to pressure gradients and elastic deformation of the surrounding tissue and local tissue damage around the needle. This infusate backflow may lead to less efficient distribution volumes and may also cause harmful side effects or complications in the untargeted surrounding regions of the infusion site [3, 5]. Its occurrence and severity can be directly correlated to several parameters including infusate viscosity, flow rate, catheter radius, and cannula tip location [4–7].

Compared to conventional cannulas which are basically narrow cylindrical tubes, devices such as microfluidic infusion probes with the fluid outlet located away from the probe edge have shown reduced backflow in tissues along the device-tissue interface [8]. “Step-down” cannulas consisting of a sharp transition from a wider cannula to a narrower tip have also been shown to reduce backflow and achieve reliable distributions in tissues [6]. Though effective, these devices may require expensive or complicated fabrication processes. Further, Guarnieri et al. [9] has proposed that the use of flexible catheters alleviates the occurrence of leak-back observed when using traditional rigid catheters. It is believed that flexible catheters provide a more consistent seal with the surrounding tissues when compared to rigid catheters. However, the use of flexible catheters may lead to difficulties in controlling the insertion path when targeting specific infusion sites. Robust and economical methods for reducing backflow during infusions are still needed.

Polymer coatings which can be applied to cannulas by simple spray processes offer another potential method to reduce backflow during infusions. In this study, dual-layer polymer coatings that swell in situ to reduce backflow were developed. Thin, bioacceptable, polymer coatings were applied along the outside surface of stainless steel cannulas prior to insertion. The coatings consist of an outside layer of poly(vinyl alcohol) (PVA) atop an underlying layer comprised of a poly(ethylene oxide) (PEO) and sodium alginate polymer mixture. These polymer coatings hydrate and swell within tissue upon insertion, creating an annular barrier to backflow along the outside track of the cannula. The coatings may also facilitate infusions near tissue surfaces, a significant limitation of current infusion techniques [10]. In vitro experiments in hydrogel tissue phantoms were conducted to examine whether backflow during infusions could be reduced significantly. In addition, experimental backflow data was fit to a model to estimate the effective compressive stress created by the swelled polymer coatings. Ex vivo experiments in excised porcine brain tissue were also conducted.

Overall, the ability of these polymers to form a seal at the infusion site during and after cannula withdrawal was investigated. Such an effect would reduce the infusate backflow which is consistently observed during uncoated cannula removal and may also prove useful

in applications requiring a bioacceptable plug to prevent fluid leakage from a target site, such as in biopsies [11–13].

## 2 Materials and methods

### 2.1 Polymer coating configuration

Water soluble polymers (WSPs) are composed of linear chains of covalent hydrophilic polymer chains that allow them to absorb surrounding liquids. When hydrated, these polymers swell and expand significantly from their dehydrated forms, and they can dissolve. With the availability of large amounts of interstitial fluid, WSP are a practical material for plug or sealing applications since they would form a gel or increased viscosity fluid along the cannula track. For this reason, WSP were chosen as the primary components for the cannula coatings with the expectation that any fluid-filled or damaged tissue regions around the cannula (which could lead to backflow) would be occupied by the hydrated polymers.

As a result of their favorable swelling properties and bioacceptability [14, 15], PEO and PVA were the primary components of the polymer coatings used in this study. Sodium alginate was mixed with PEO to serve as a thickening agent, increasing the viscosity, and therefore increasing the resistance to any backflow that may occur inside the polymers themselves when hydrated. These polymers were applied to the cannulas in a dual-layered coating configuration. Relative to preliminary optimization trials using single-layered coatings consisting of one or a blend of WSP, the dual-layered coating of the above polymers proved to be more effective in preventing backflow. The first inner layer consisted of a PEO and alginate mixture which quickly formed a viscous gel when hydrated. Given its high viscosity and rapid swelling behavior, this inner layer served as the primary resistance to infusate backflow. The second top layer of PVA hydrated more slowly and therefore shielded the inner PEO layer from excess exposure to surrounding water during insertion. Without this outside layer of PVA, the unprotected PEO layer did not have mechanical integrity and was found to slide off the cannula surface before reaching the target site.

### 2.2 Polymer coating application onto cannulas and coating characterization

For all infusions, 28 gauge (0.36 mm) outer diameter stainless steel cannulas (7762-02 *Hamilton Company, Reno, Nevada*) were used. Each cannula was initially coated with a 3 % (w/v) PEO (~600,000  $M_w$ , *Sigma Aldrich, St. Louis, MO*) and 0.5 % (w/v) sodium alginate (~250 cps, *Sigma Aldrich, St. Louis, MO*) mixture, followed by a top layer of 7 % (w/v) PVA (~86,000  $M_w$ , *Acros Organics, Geel, Belgium*) solution. To differentiate between polymer layers during application and in image analysis, green and red food coloring was added to the PVA and PEO/alginate solutions, respectively. Each coating, or layer, of polymer was sprayed repeatedly onto individual cannulas using a gravity feed airbrush (*TCP-Global, San Diego, CA*) held 3 in. away from the cannula surface. Cannulas were rotated by hand throughout the spraying process and were dried every 5 s using a heat gun placed 7 in. away from the cannula. The use of the heat gun at a distance shorter than 7 in. and for a drying period longer than 5 s often resulted in increased coating surface roughness due to the violent evaporation of water vapor from the polymer coating solution applied. After applying the coatings, the cannulas were left to dry overnight (8–9 h) in a vacuum oven set to 60 °C. To quantify the thickness of each dry polymer layer, scanning electron microscopy was used to take images of cannulas with and without polymer coatings (Fig. 1). The difference in thickness between the coated and non-coated cannula was assessed with digital image analysis via the conversion of image pixels to microns found using the diameter of the cannula as a known measurement reference.

Once hydrated within the tissue phantom, total polymer swelling thickness measurements were generated by averaging the total diameter created by the hydrated polymers along a 10 mm section from the edge of the polymer coating closest to the cannula tip. This method was chosen due to the unevenness of the hydrated coatings. The outer cannula diameter (0.36 mm) was subtracted from this average and the resulting difference was divided in half to calculate average thickness of the hydrated polymer coating. Refer to Fig. 2 for a schematic of the implanted cannula.

### 2.3 In vitro infusion testing

All in vitro infusions were conducted in a hydrogel tissue phantom prepared using a 0.6 % (w/v) solution of Trevi-Gel™ 5000 powder (*Trevigen, Gaithersburg, MD*) in distilled water [16]. The solution was covered and heated to boiling over a hot plate. After boiling, the solution was poured into a 40 × 60 × 25 mm acrylic cast and the solution solidified as it approached room temperature. The infusion cannulas were connected via non-compliant polymer tubing to a syringe pump. Cannulas were carefully inserted into the hydrogel brain tissue phantom to a distance of 25 mm using a stereotactic guide (*Graduated Knob UniSlide, Velmex, Bloomfield, NY*). The stereotactic guide was calibrated in two orthogonal planes to ensure straight entrance of the cannula into the tissue phantoms. After insertion into the tissue phantom, cannulas were allotted 8–10 min to allow for the hydration of the PEO/alginate and PVA coatings. Preliminary tests showed that a waiting time of 8 min allowed the polymer coatings to hydrate and expand considerably while maintaining a high enough viscosity to resist backflow throughout infusions. Immediately after this hydration period, 4.0 µl of Evans Blue labeled albumin (EBA) was infused into the phantom at constant flow rates, 0.3, 0.4, 0.5, and 0.6 µl min<sup>-1</sup>. This range was chosen because previous trials for this setup showed that infusate backflow consistently occurred during control experiments using non-coated stainless steel cannulas at infusion rates of 0.3 µl min<sup>-1</sup> and greater. The experiments were performed for polymer-coated cannulas (n = 6) and uncoated cannulas (n = 6) at each flow rate. Images were taken every 30 s using a CMOS camera (*OptixCam Summit Series OCX-5, Wirtz, VA*) with an attached ×4 magnification imaging lens stationed directly above the tissue phantom cast. Backflow distances, which were defined as the total longitudinal distance traveled by the EBA infusate along the outside of the cannula, were measured.

### 2.4 Ex vivo infusion testing

Ex vivo experiments were performed in excised porcine brain tissue obtained from the University of Florida slaughterhouse in accordance with UF animal care guidelines. The tissue was kept at low temperature within an ice box to slow tissue degeneration prior to experimentation which was conducted within 1.5–4 h of tissue slicing (including transportation, set-up, and infusion experiments). The experiments consisted of control infusions using 28 gauge (0.36 mm OD) uncoated stainless steel needles (n = 7) and cannulas with the same dual-layered polymer coating (n = 7). The radiatio corporis callosi, a large white matter region, was chosen as the infusion site [17]. Cannula insertion was from the brain surface and the arachnoid membrane was partially removed to allow for easy insertion before all infusion experiments. The route of the cannula was approximately in the coronal plane. Due to the softness of brain tissue, tissue samples were also supported with 0.6 % hydrogel within an acrylic cast (~1 h to prepare and solidify). The infusion system used was identical to that used for in vitro testing. After cannula insertion, a 5–7 min waiting time was allotted and 4.0 µl EBA was infused at a rate of 0.3 µl min<sup>-1</sup>. At the end of infusion, the cannula was slowly removed from the tissue sample. After completion of infusions, brain tissue was sectioned ~5 mm from the infusion site through a plane parallel with the cannula to check for backflow. Backflow distances were not quantitatively

evaluated as the cannula tip location could not be determined after the removal of the cannula.

## 2.5 Residual stress estimates

A simple analytical model was also used to estimate local polymer coating and tissue interactions which result in compressive residual stresses surrounding the cannula and which otherwise cannot be measured experimentally. Previously developed backflow models [7, 18] were adapted to account for a residual stresses between the cannula and surrounding media. Then calculated backflow distances were compared to experimental measures ( $n = 6$ ) to estimate an equivalent residual stress ( $\sigma_r$ ) for polymer-coated needles. Previous backflow models considered tissue surrounding a cylindrical cannula (modeled using an axis-symmetric geometry) with tissue behaving as linear elastic porous media. Fluid was allowed to enter between the porous media and cannula producing a gap between the tissue and the outer cannula wall. The flow through the gap was considered to follow Poiseuille's law and expansion of the gap produced stress in the surrounding porous media. In this study, the stress generated by the polymer swelling was considered as a residual stress that infused fluid had to overcome before backflow was generated. Therefore with backflow, it was assumed that infusion pressure equals  $\sigma_r$  in the porous media (polymer plus tissue) at the cannula boundary. Also, the bulk of infusion was assumed to take place along the cylindrical surface surrounding the cannula, and the pressure along the cannula length was supposed to be constant rather than decreasing with distance from the cannula tip. (This assumption was based on tracer distribution patterns which show approximately constant penetration depths along the cannula track, see Figs. 3 and 6.) Based on the backflow model of Morrison et al. [7], the residual stress needed to infuse at a flow rate  $Q$  is then given by

$$\sigma_r = \frac{Q}{Z2\pi\phi k} \ln \left( \frac{L}{r_c} \right) \quad (11)$$

where  $Z$  is the backflow distance,  $r_c$  is the outside radius of the cannula,  $L$  is the characteristic length,  $\phi$  is the porosity, and  $k$  is the hydraulic conductivity of the surrounding porous media tissue. Values of  $L = 4$  cm,  $k = 6 \times 10^{-9}$  cm<sup>4</sup>/dyne s [18], and  $\phi = 0.6$  [19] were used based on previously reported values for hydrogel. The experimental values of  $z$  where calculated in Eq. (11) for varying  $Q$  and  $\sigma_r$  to estimate varying residual stress loading. A sensitivity analysis was done to evaluate the influence of this preload on the backflow distances. Residual stresses were also estimated using the backflow model of Raghavan et al. [18] considering  $\sigma_r$  to equal the infusate pressure at the far end of the backflow region, and similar results were obtained. Best fit values for  $\sigma_r$  were determined using the least squares method.

## 3 Results

### 3.1 Polymer coating measurements

For coated needles prior to insertions, the inner PEO/alginate layer was found to range from 25 to 30  $\mu\text{m}$  and the outer PVA layer was determined to be less than 5  $\mu\text{m}$ . Before vacuum oven drying, the PEO/alginate layer was found to have a mass of  $2.34 \pm 0.24$  mg ( $n = 10$ ) and the mass of the PVA layer was  $1.60 \pm 0.23$  mg ( $n = 10$ ). Since this top layer was used solely as a protective cover for the inner coating, only a very thin coating was needed. After drying in the vacuum oven, the total mass of the polymer dual layer on the cannulas was reduced to  $3.18 \pm 0.26$  mg ( $n = 10$ ). After the set hydration period during infusions, the swelling of the polymers was generally non-uniform (conforming to surrounding free spaces) along the cannula with an average thickness of 0.37 mm from the cannula surface ( $n = 10$ ).

### 3.2 In vitro infusions

Infusions performed using uncoated cannulas consistently had significant amounts of backflow at each infusion rate tested. This backflow occurred immediately following the start of infusions and reached a distance of 18 mm on average from the tip of the cannula, resulting in little to no spread within the target site at the tip of the cannula (Fig. 3a). Under the same conditions, the dual-layered polymer coating of the PEO/alginate mixture and PVA provided more successful distributions (Fig. 3b). These infusate distributions generally took an elliptical shape, elongated along the major axis of the cannula in the direction of insertion. Occasionally, distributions would take an irregular shape, the most common of which included a narrow leak-back, or “tail,” of infusate often along only one side of the cannula (Fig. 3c). As shown in Fig. 4 and Table 1, average backflow distance with coated cannulas was reduced by ~83 % to 3.1 mm at an infusion rate of  $0.3 \mu\text{l min}^{-1}$  when compared to that of the uncoated cannulas (18 mm). As the infusion rate was increased to  $0.6 \mu\text{l min}^{-1}$ , average backflow distances were found to increase to 11.4 mm at the highest flow rate tested. This still corresponds to a 37 % reduction when compared to the 18 mm average backflow distances observed when using uncoated cannulas.

Upon insertion, the behavior of the polymer coatings showed minor variations between trials. For ~75 % of the insertions, the polymer coatings slid greater than 1 mm away from the cannula tip due to early hydration of the inner PEO layer near the tip (Fig. 3b). This “slipped” distance was 2.6 mm on average and reached a maximum of 8.6 mm. The coatings of the remaining ~25 % of the cannulas tested stayed attached within 1 mm of the tip during the entire insertion. Swelling behaviors, such as the time needed for hydration and the thickness upon hydration, were not affected by these slipped variations.

General trends depict a decreased backflow distance with increased polymer slipping (Fig. 5a). The slipped polymers were found to accumulate at a certain distance along the outside of the cannula track, forming a dense wall. The mechanisms by which backflow was impeded in this slipped case occurred in two forms. In the most reoccurring of these two forms, backflow was prevented immediately upon contact with the polymer wall (Fig. 5b). For the latter of the two forms, backflow was prevented directly at the tip, without direct contact with the accumulated polymers further down the cannula (Fig. 5c). For infusions with no polymer coating detachment, the reduction of backflow began immediately at the tip of the cannula upon contact with the hydrated coating (Fig. 6a). Lastly, backflow along the cannula track was repetitively observed upon removal of uncoated cannulas from the hydrogel tissue phantom after an insertion. In contrast, the hydrated polymers from the coatings remained within the needle cavity upon withdrawal of coated needles, forming a resistant plug at the edge of the infusion site and keeping the injected EBA in place (Fig. 6b). This phenomenon occurred only if the top PVA layer was inserted entirely into the tissue media (with no portion protruding from the outside tissue phantom surface) and allowed to hydrate completely ( $t > 15 \text{ min}$ ).

### 3.3 Ex vivo infusions

Porcine brain infusions also resulted in successful reduction of backflow. In the control trials, use of needles with no polymer coating resulted in considerable backflow for every case with ~57 % of these leak-backs reaching the outside tissue surface. A typical backflow along the cannula is shown in Fig. 7a. In trials with the coated needles, the polymers significantly reduced the backflow for every infusion as determined from tissue slices. Figure 7b shows a typical distribution observed when using coated needles. The final tracer distributions in tissue were often elliptical along the major axis of the cannula. In comparison to the hydrogel studies, ~86 % of tissue infusions exhibited an increased

occurrence of the previously mentioned backflow “tails”. This slight backflow around the infusion site was small when compared to that of uncoated cannulas.

### 3.4 Residual stress

For in vitro hydrogel tests, the estimated value for the residual stress around the needle was 0.252 kPa based on both the experimental and predicted values for backflow. As seen in Fig. 4, it can be observed that with no residual stress, backflow models predict a backflow distance greater than 15 mm; whereas with a residual stress introduced by polymer swelling, the calculated values provide a reasonable approximation of the experimental values ( $R^2 = 0.82$ ). This sensitivity analysis showed that for low values of  $\sigma_r$ , a small increase in compressive residual stress produced an important reduction of the backflow distances. However, with high residual stresses ( $\sigma_r > 0.4$  kPa), any further increase produced only a slight decrease in the backflow distance, and the backflow distance did not depend on the infusion flow rate over the range tested.

## 4 Discussion

In this study, a new cannula design for preventing infusate backflow was assessed. Surface coatings of WSPs were tested in vitro and ex vivo to see if they maintain structural integrity during cannula insertion and successfully swell to prevent backflow. The choice of polymers to use for the coating was directed by looking for a safe and effective material. There is a limited pool of synthetic polymers that form hydrogels, and have been used for implantable applications. First attempts on creating the cannula coatings focused on the application of single polymer layers. Dextran, polyvinyl pyrrolidone, PVA, PEO, and sodium alginate were the polymers used in preliminary single layer trials. Except for PVA, all of the above polymers showed slip off the needle upon insertion and did not reach the target infusion site. However, PEO showed a much larger expansion upon hydration in comparison to other polymers. For this reason, PEO was chosen as the primary polymer for the inner cannula coatings. Being the slowest hydrating polymer and the least likely to slip in these single layer trials, PVA was applied on top of the PEO layer to protect the inner layer from early hydration and excessive slipping. Sodium alginate was added to the inner PEO layer to increase the viscosity of the hydrated inner coating and prevent the backflow that at times occurred within this inner layer. The relative amounts of PVA, PEO, and sodium alginate used in this study were optimized to achieve the smallest backflow distances. Overall, the dual polymer layer formulation presented allows for a controlled hydration that was difficult to achieve with a single layer coating. By providing a thin outer coating of the slowly hydrating PVA, the inner layer of PEO and alginate was able to avoid early hydration and reach the target site without completely detaching from the cannula. The high viscosity of this inner PEO/alginate layer was the primary contributing factor in resisting infusate backflow. It is likely that other polymer compositions would work for this application as well, to successfully hinder backflow.

Alginate, PEO and PVA (soluble, not crosslinked) are generally considered to be biocompatible. Alginate is commonly used to suspend and encapsulate therapeutic cells without apparent cytotoxicity [20–22]. Intraperitoneal (ip) administration of low doses (25 or 50 mg/kg) of alginate solutions reportedly improved experimentally induced glomerulonephritis in rats [23], and intravenous (iv) injections of 0.2 % alginate solutions had a reported antiedematous effect in dogs with experimentally induced brain edema [24]. Another study reports that ip or iv injections of alginate ( $\sim 200,000$  g/mol  $M_w$ ) in mice caused “no untoward effects” [25]. However, iv administration of high doses ( $\sim 100$  mg/kg) of alginate ( $\sim 85,000$  g/mol  $M_w$ ) were lethal to mice, rabbits and cats [26]; ip or iv administration of similarly high doses of alginate or alginic acid were also lethal to cats [27]. No adverse events were observed in rats receiving iv injections of 0.01 and 0.025 % PEO

(4,000,000 g/mol  $M_w$ ) solutions in a 4 ml (4 and 10 mg/kg, respectively) dose [28]. Injections of 2.5 ml of 0.05 % PEO or 0.3 ml of 0.10 % PEO (12.5 and 3.0 mg/kg, respectively) caused death however; intense mechanical shearing of the 0.10 % PEO solution to reduce solution viscosity via degradation of the PEO  $M_w$  abrogated this acute toxicity, even for high doses (40 mg/kg) [28]. In concert with these findings, polyethylene glycol (i.e., lower  $M_w$  PEO) has a reported very low toxicity in animal studies [29] and a therapeutic protective effect in the injured brain and spinal cord [30–33]. Iv injections of radio-labeled PVA solutions into mice were not associated with acute toxicity; lower  $M_w$  PVA (<100,000 g/mol) was more rapidly cleared from the blood by the kidney while higher  $M_w$  PVA (>100,000 g/mol) had a long half-life in the blood and showed increased accumulation in the liver [34]. Adverse events were not reported after ip administration of 0.1 ml, 5 wt% PVA (195,000 g/mol  $M_w$ ) solutions to rabbits and nude mice; PVA was excreted by the kidney over many days without causing apparent organ damage [35]. Given all this previously reported data, it is expected that the polymer sizes ( $M_w$ ) and amounts used as described here pose little risk (if any) of toxicity (local or systemic) and are therefore bioacceptable/biocompatible for the described use. However, further in vivo testing will be required to determine any specific inflammation response to these polymer coatings as well as their long term biocompatibility.

The dual-layered coatings comprising of these WSPs resulted in significant backflow reductions in comparison to control experiments with uncoated cannulas during in vitro hydrogel and excised tissue infusions. Moreover, the polymers continued to demonstrate this preventative effect even after cannula withdrawal by filling the space left by the cannula. In these in vitro studies, variations in polymer swelling and slipping behavior were observed within infusion trials, but none showed an obvious negative impact on backflow reduction. Also, experimental results showed that increasing the slip distance of these polymer coatings along the cannula during insertion resulted in a slight decreasing trend with backflow distance (Fig. 5a). It was observed that this slipping distance was highly dependent on the amount of PVA that was applied around the PEO/alginate inner layer. If a thinner or less consistent PVA layer was applied, it was more likely that the inner PEO/alginate layer partially hydrated during the insertion, losing its solidity and forming a viscous gel that could slide backward along the needles surface due to the opposing shear forces of the surrounding hydrogel walls. This effect is also closely tied to the insertion rate of the cannula, with slower rates leading to increased polymer hydration and sliding during insertions. The polymer formulation presented can be easily adjusted to allow for early or delayed hydration depending on the particular application or surgical method used.

The current spraying method used to apply the polymers to the cannula resulted in non-smooth surfaces, Fig. 1. Surface roughness may increase the friction, tearing, or deformation of tissue along a cannula track during insertion. Non-uniform coatings may have also contributed to the varying hydration and slipping behaviors observed in this study. Inconsistency of the outer PVA layer may also leave the inner layer exposed on some surfaces along the cannula which would speed up the hydration process and result in non-uniform thickness. Even without highly uniform coatings, significant backflow reduction was observed compared to controls. Alternative coating application techniques as well as the specific impact of polymer surface smoothness and thickness on backflow reduction may be evaluated in future studies. It should also be noted that hydrogels used in these in vitro studies were not equilibrated in physiological solution which may affect the extent of hydrogel swelling. Future studies will determine changes in polymer swelling behavior in vivo.

The overall slipped polymer configuration found in this study showed some resemblance to the silica “step-down” cannula developed by Yin et al. [6], in that the sharp transition from



the diameter of the bare cannula to the effective diameter of the hydrated coatings served as a barrier to backflow. Advantages of the polymer coatings in comparison to step-down cannulas are their ability to conform to the surrounding tissue and remain within the cavity after the withdrawal of the cannula. While hydrating, the coatings have the ability to apply compressive stresses to surrounding tissues and fill the free spaces around the cannula caused by misalignment or damage. It must be noted that the swelling of the current polymer coating formulation increased the overall cannula diameter considerably. As a result the potential for tissue damage in surrounding tissues may be greater than other techniques and further in vivo studies may investigate effects of tissue compression on secondary side effects. The backflow models used in this study predicted residual stress values which could not otherwise be measured. The compressive stresses estimates within hydrogel tissue phantoms were predicted to be quite low (~0.754 kPa). In vivo stresses within soft tissues with similar mechanical stiffness should be on the same order of magnitude. The porous media models used to estimate backflow made several simplifying assumptions, including that WSP coatings and the hydrogel tissue phantom had similar mechanical and transport properties. Also, preexisting gaps and hydrogel damage due to needle insertion were considered negligible. Future models can be adapted to consider these effects.

In the hydrogel studies, the backflow of EBA was not only stopped upon reaching the slipped polymer wall, but was also observed at times to end before even reaching the polymer coating. It is possible that the accumulated polymer wall formed a seal along the cannula interface that did not allow any pressure difference to form along the surface of the cannula from the tip to the atmospheric interface. This effect may be caused by a compacted region created within the surrounding media upon insertion and swelling. These effects may also occur in tissues, however, detailed backflow or polymer slipping behavior during infusions into the excised tissue could not be recorded due to the tissue's lack of transparency.

Ex vivo experiments showed promising results, but some limitations should be noted. These tissue infusions did not reflect the exact mechanics of live tissue which may affect the behavior of the polymers. For example, the effect of blood vessel damage could not be observed in these trials. Further, extracellular spaces shrink in excised tissue samples and tissues degrade with necrosis. Thus, infusion transport may not be the same during in vivo infusions [36]. Also, these excised tissue samples may also not accurately represent the fluid content of live tissue. Although tissue samples were kept hydrated by surrounding hydrogel, they did not have the circulating blood flow of living tissues. Future experiments will be conducted in vivo to test these polymer coatings.

## 5 Conclusion

This study presents a simple dual-layered polymer coating technology that can be used to minimize or eliminate the occurrence of infusate backflow during direct tissue infusion. In vitro hydrogel and excised tissue experiments showed that the hydration of these applied polymer coatings over a period of time forms a resistive annular barrier that impedes the leak-back of infusate. These polymer-coated cannulas have several advantages over alternative, more complex devices proposed for the reduction of backflow during infusions. They have a simple design and would be relatively easy to produce since they do not require complex or costly manufacturing processes. Another difference of this device is that the hydrated coatings remain in place after cannula withdrawal and form a biocompatible plug that continues to prevent backflow. The coatings can therefore be applied to several applications where a bioacceptable seal is needed. One example includes tumor biopsies, where the leak-back and migration of cancer cells during cannula withdrawal is a significant concern. This technology may also allow injections near tissue surfaces or interfaces which

is a current limitation of CED within CNS tissues. An important characteristic of the simple polymer-coated cannula presented in this study is its ability to conform to the surrounding tissue after insertion and create an effective seal. Future work will further assess the effectiveness of these coatings in preventing backflow in vivo as well as biocompatibility of the polymer coatings.

## Acknowledgments

We would like to thank Ronja Maånsson for her preliminary work on this project as well as Gregory Pishko and Benjamin Oberstein for their assistance in the construction of the current experimental infusion setup. The project described was supported by award number R01NS063360 from the National Institute of Neurological Disorders and Stroke. The content is solely the responsibility of the authors and does not necessarily represent the official views of the National Institute Neurological Disorders and Stroke or the National Institutes of Health. This work was also supported in part by NIH/NCRR CTSA award to the University of Florida UL1 RR029890, as well as the University Scholars Program, University of Florida.

## References

- Bobo RH, Laske DW, Akbasak A, Morrison PF, Dedrick RL, Oldfield EH. Convection-enhanced delivery of macromolecules in the brain. *Proc Natl Acad Sci USA*. 1994; 91(6):2076–2080. [PubMed: 8134351]
- Gill SS, Patel NK, Hotton GR, O’Sullivan K, McCarter R, Bunnage M, et al. Direct brain infusion of glial cell line-derived neurotrophic factor in Parkinson disease. *Nat Med*. 2003; 9(5):589–595. [PubMed: 12669033]
- Rogawski MA. Convection-enhanced delivery in the treatment of epilepsy. *Neurotherapeutics*. 2009; 6(2):344–351. [PubMed: 19332329]
- Sampson JH, Brady ML, Petry NA, Croteau D, Friedman AH, Friedman HS, et al. Intracerebral infusate distribution by convection-enhanced delivery in humans with malignant gliomas: descriptive effects of target anatomy and catheter positioning. *Neurosurgery*. 2007; 60(2):89–98.
- Chen MY, Lonser RR, Morrison PF, Governale LS, Oldfield EH. Variables affecting convection-enhanced delivery to the striatum: a systematic examination of rate of infusion, cannula size, infusate concentration, and tissue-cannula sealing time. *J Neurosurg*. 1999; 90(2):315–320. [PubMed: 9950503]
- Yin D, Forsayeth J, Bankiewicz KS. Optimized cannula design and placement for convection-enhanced delivery in rat striatum. *J Neurosci Methods*. 2010; 187(1):46–51. [PubMed: 20026357]
- Morrison PF, Chen MY, Chadwick RS, Lonser RR, Oldfield EH. Focal delivery during direct infusion to brain: role of flow rate, catheter diameter, and tissue mechanics (vol 277, pg R1218, 1999). *Am J Physiol Regul Integr Comp Physiol*. 2002; 282(6):R1218–R1229.
- Neeves KB, Lo CT, Foley CP, Saltzman WM, Olbricht WL. Fabrication and characterization of microfluidic probes for convection enhanced drug delivery. *J Control Release*. 2006; 111(3):252–262. [PubMed: 16476500]
- Guarnieri M, Carson BS, Khan A, Penno M, Jallo GI. Flexible versus rigid catheters for chronic administration of exogenous agents into central nervous system tissues. *J Neurosci Methods*. 2005; 144(2):147–152. [PubMed: 15910972]
- Jagannathan J, Walbridge S, Butman JA, Oldfield EH, Lonser RR. Effect of ependymal and pial surfaces on convection-enhanced delivery. Laboratory investigation. *J Neurosurg*. 2008; 109(3): 547–552. [PubMed: 18759589]
- Cho MH, Malhotra A, Donahue DM, Wain JC, Harris RS, Karpaliotis D, et al. Mechanical ventilation and air leaks after lung biopsy for acute respiratory distress syndrome. *Ann Thorac Surg*. 2006; 82(1):261–267. [PubMed: 16798226]
- Kelley ML, Mosenthal WT, Milne J. Bile leakage following menghini needle liver biopsy. *J Am Med Assoc*. 1971; 216(2) 333–333(1).
- Wiksell H, Schassburger KU, Janicijevic M, Leifland K, Lofgren L, Rotstein S, et al. Prevention of tumour cell dissemination in diagnostic needle procedures. *Br J Cancer*. 2010; 103(11):1706–1709. [PubMed: 21045831]

14. Bjugstad KB, Lampe K, Kern DS, Mahoney M. Biocompatibility of poly(ethylene glycol)-based hydrogels in the brain: an analysis of the glial response across space and time. *J Biomed Mater Res A*. 2010; 95A(1):79–91. [PubMed: 20740603]
15. Jiang YJ, Schadlich A, Amado E, Weis C, Odermatt E, Mader K, et al. In vivo studies on intraperitoneally administrated poly(vinyl alcohol). *J Biomed Mater Res B*. 2010; 93B(1):275–284.
16. Chen ZJ, Gillies GT, Broaddus WC, Prabhu SS, Fillmore H, Mitchell RM, et al. A realistic brain tissue phantom for intraparenchymal infusion studies. *J Neurosurg*. 2004; 101(2):314–322. [PubMed: 15309925]
17. Felix B, Leger ME, Albe-Fessard D. Stereotaxic atlas of the pig brain. *Brain Res Bull*. 1999; 49(1–2):1–137. [PubMed: 10466025]
18. Raghavan R, Mikaelian S, Brady M, Chen ZJ. Fluid infusions from catheters into elastic tissue: I. Azimuthally symmetric backflow in homogeneous media. *Phys Med Biol*. 2010; 55(1):281–304. [PubMed: 20009198]
19. Chen XM, Astarly GW, Sepulveda H, Mareci TH, Sarntinoranont M. Quantitative assessment of macromolecular concentration during direct infusion into an agarose hydrogel phantom using contrast-enhanced MRI. *Magn Reson Imaging*. 2008; 26(10):1433–1441. [PubMed: 18583082]
20. Lim F, Sun AM. Microencapsulated islets as bioartificial endocrine pancreas. *Science*. 1980; 210(4472):908–910. [PubMed: 6776628]
21. Soonshiong P, Feldman E, Nelson R, Heintz R, Yao Q, Yao ZW, et al. Long-term reversal of diabetes by the injection of immunoprotected islets. *Proc Natl Acad Sci USA*. 1993; 90(12):5843–5847. [PubMed: 8516335]
22. Soonshiong P, Heintz RE, Merideth N, Yao QX, Yao ZW, Zheng TL, et al. Insulin independence in a type-1 diabetic patient after encapsulated islet transplantation. *Lancet*. 1994; 343(8903):950–951. [PubMed: 7909011]
23. Mirshafiey A, Borzooy Z, Abhari RS, Razavi A, Tavangar M, Rehm BHA. Treatment of experimental immune complex glomerulonephritis by sodium alginate. *Vasc Pharmacol*. 2005; 43(1):30–35.
24. Lavrov VP. The experimental treatment of acute edema of the brain with sodium alginate From: *Ref Zh Otd Vypusk Farmakol Toksikol*, 1964, no. 22.54.98 (translation). *Sb Nauch Tr Vladi Vostokskh Med Inst*. 1964; 2(1):9–10.
25. Hagen A, Skjak-Braek G, Dornish M. Pharmacokinetics of sodium alginate in mice. *Eur J Pharm Sci*. 1996; 4(Suppl) 100–100(1).
26. Solandt OM. Some observations upon sodium alginate. *Q J Exp Physiol Cogn Med Sci*. 1942; 31:25–30.
27. Chenoweth MB. The toxicity of sodium alginate in cats. *Ann Surg*. 1948; 127(6):1173–1181. [PubMed: 17859157]
28. Smyth HF, Weil CS, Woodside MD, Knaak JB, Sullivan LJ, Carpenite CP. Experimental toxicity of a high molecular weight poly(ethylene oxide). *Toxicol Appl Pharmacol*. 1970; 16(2):442–445. [PubMed: 5435611]
29. Fruijtier-Polloth C. Safety assessment on polyethylene glycols (PEGs) and their derivatives as used in cosmetic products. *Toxicology*. 2005; 214(1–2):1–38. [PubMed: 16011869]
30. Borgens RB, Shi R. Immediate recovery from spinal cord injury through molecular repair of nerve membranes with polyethylene glycol. *FASEB J*. 2000; 14(1):27–35. [PubMed: 10627277]
31. Shi R, Borgens RB. Acute repair of crushed guinea pig spinal cord by polyethylene glycol. *J Neurophysiol*. 1999; 81(5):2406–2414. [PubMed: 10322076]
32. Shi R, Borgens RB. Anatomical repair of nerve membranes in crushed mammalian spinal cord with polyethylene glycol. *J Neurocytol*. 2000; 29(9):633–643. [PubMed: 11353287]
33. Smucker P, Hekmatyar SK, Bansal N, Rodgers RB, Shapiro SA, Borgens RB. Intravenous polyethylene glycol successfully treats severe acceleration-induced brain injury in rats as assessed by magnetic resonance imaging. *Neurosurgery*. 2009; 64(5):984–990. [PubMed: 19404158]
34. Tabata T, Murakami Y, Ikada Y. Tumor accumulation of poly(-vinyl alcohol) of different sizes after intravenous injection. *J Control Release*. 1998; 50(1–3):123–133. [PubMed: 9685879]

35. Jiang YJ, Schadlich A, Amado E, Weis C, Odermatt E, Mader K, et al. In vivo studies on intraperitoneally administrated poly(vinyl alcohol). *J Biomed Mater Res B*. 2010; 93B(1):275–284.
36. Nicholson C, Sykova E. Extracellular space structure revealed by diffusion analysis. *Trends Neurosci*. 1998; 21(5):207–215. [PubMed: 9610885]

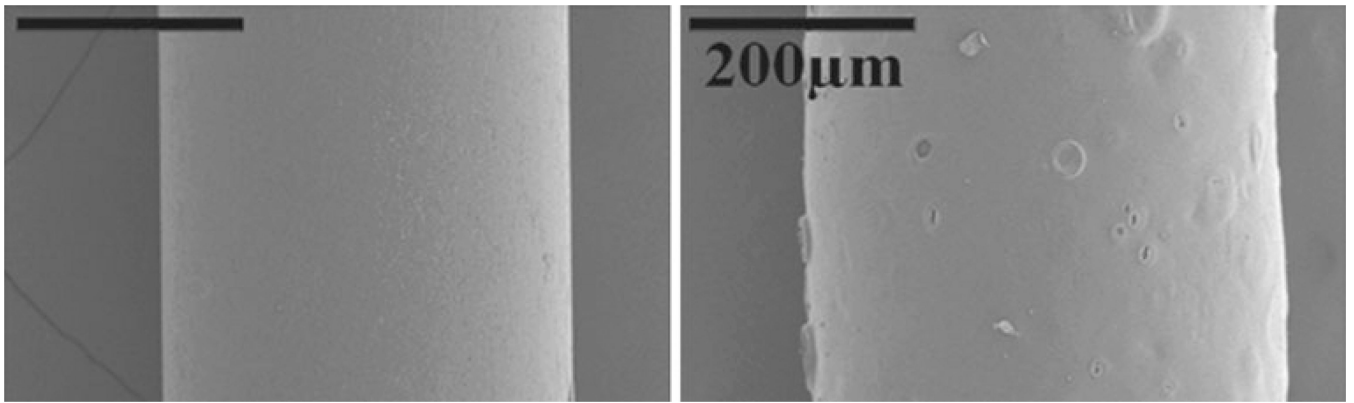


**Fig. 1.** SEM image of a non-coated (*left*) and dual-layered polymer-coated cannula (*right*). The dehydrated coating thickness was found to range from 30 to 35  $\mu\text{m}$

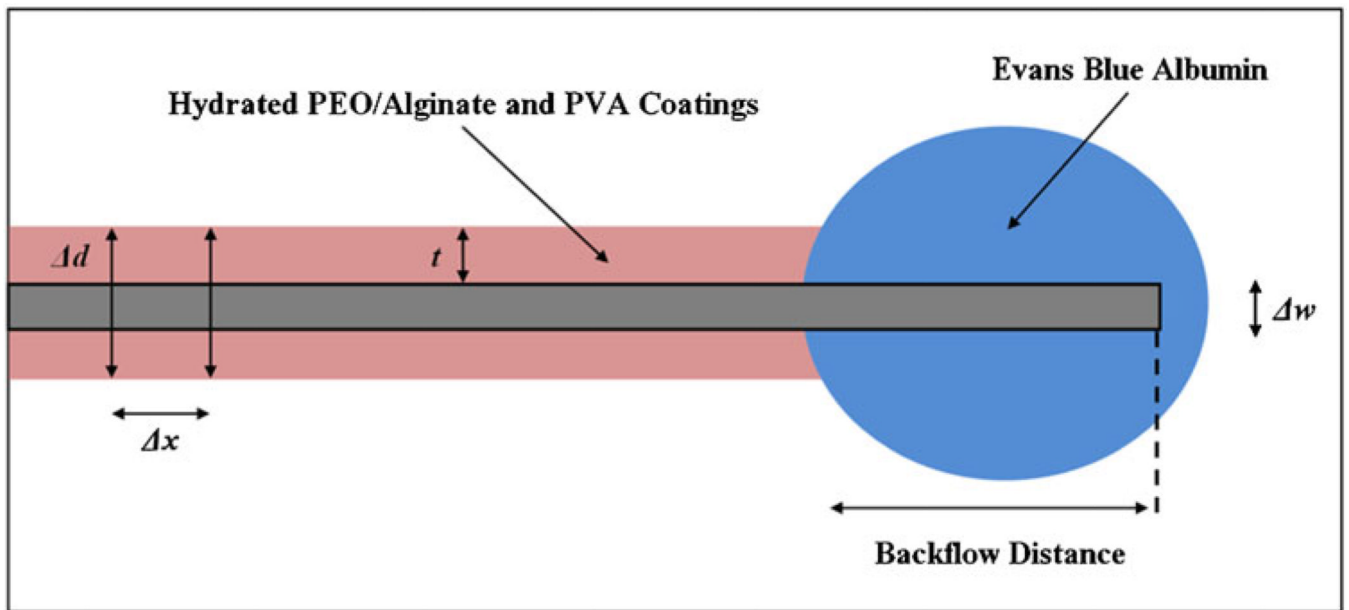


**Fig. 2.** A schematic depiction of polymer swelling and backflow distance. Polymer swelling thickness measures were made by averaging the total diameters ( $\Delta d$ ) of the hydrated polymers along a 10 mm section from the edge of the polymer coating closest to the cannula tip. Measurements were taken at 1 mm intervals ( $\Delta x$ ). The cannula width was then subtracted from the total diameter average and the resultant polymer-only distance was divided in half to represent the thickness along one side ( $t$ ). Backflow distances were measured from the tip of the cannula to the leading tracer edge along the cannula

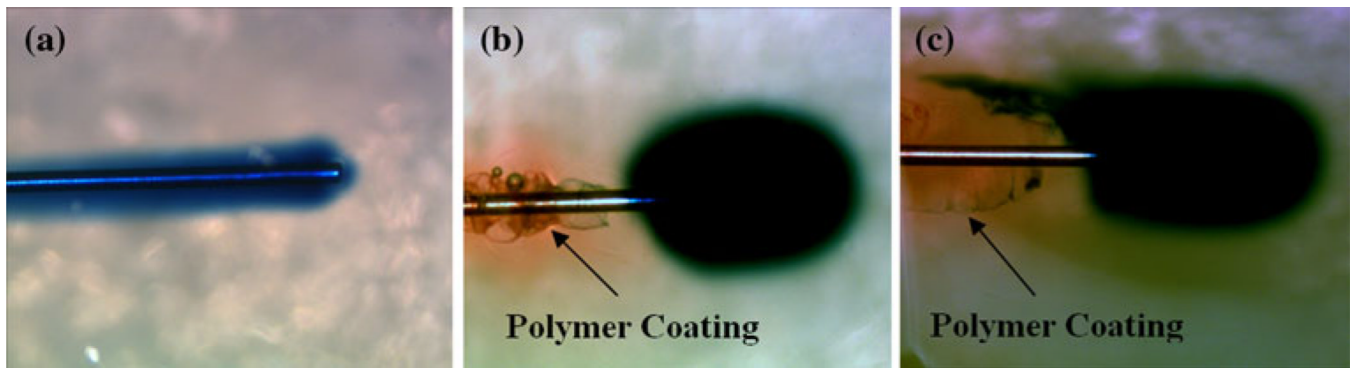


**Fig. 3.** Hydrogel infusion experiment. **a** Severe backflow using uncoated cannulas during infusions of  $0.3 \mu\text{l min}^{-1}$ . **b** Severe backflow was eliminated at an infusion rate of  $0.3 \mu\text{l min}^{-1}$  giving a near spherical distribution with polymer-coated cannula (hydrogel colored *red*). **c** In some instances backflow is reduced but with a tracer “tail” emerging along narrow ridges on the outside of the polymer coating (Color figure online)

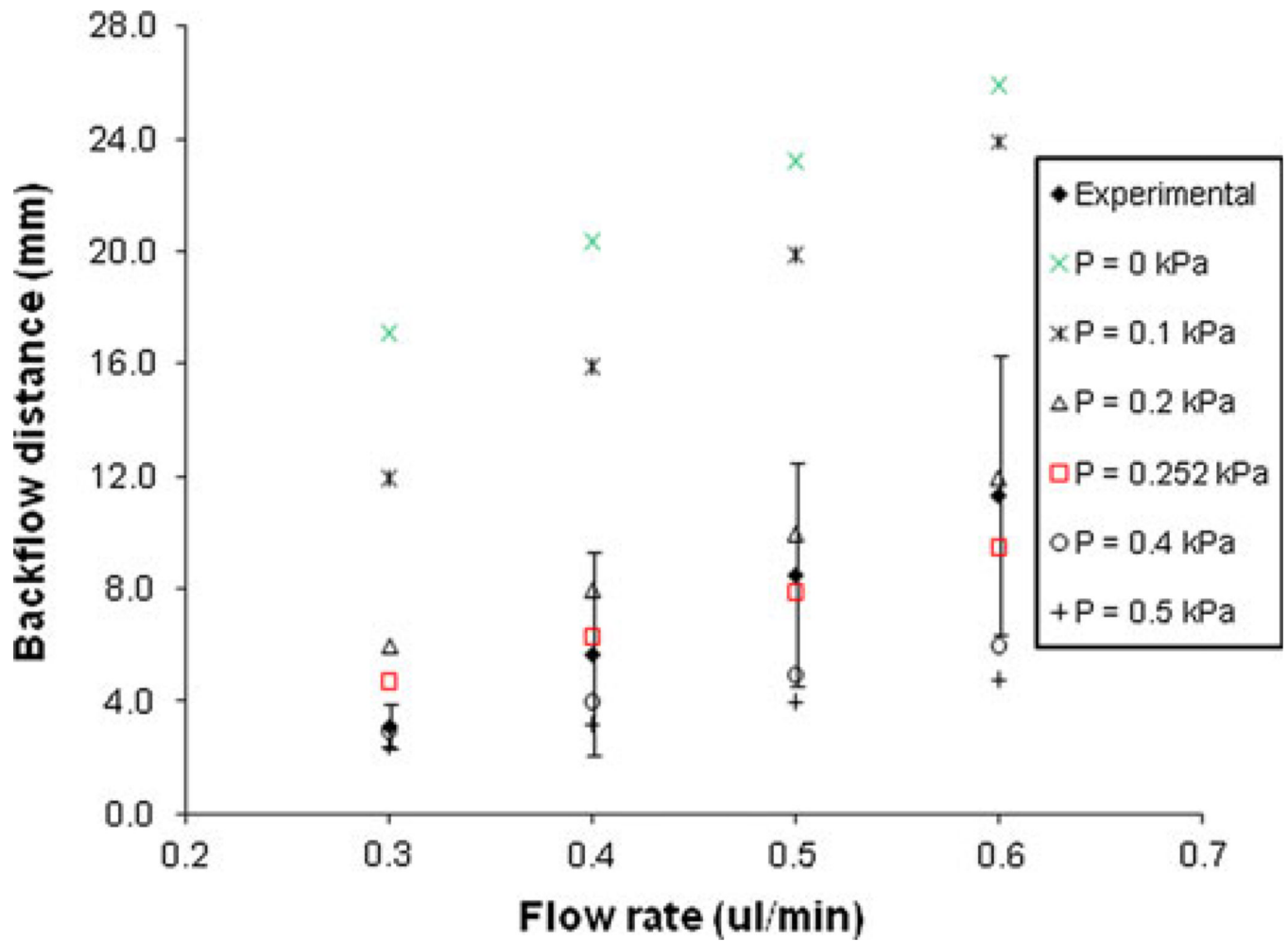


**Fig. 4.** Effect of compressive residual stresses surrounding the cannula on backflow distance within the hydrogel tissue phantom. Experimental backflow data from hydrogel tests was compared to backflow model predictions to estimate the residual stress. The estimated value for the residual stress was 0.252 kPa with  $R^2 = 0.82$



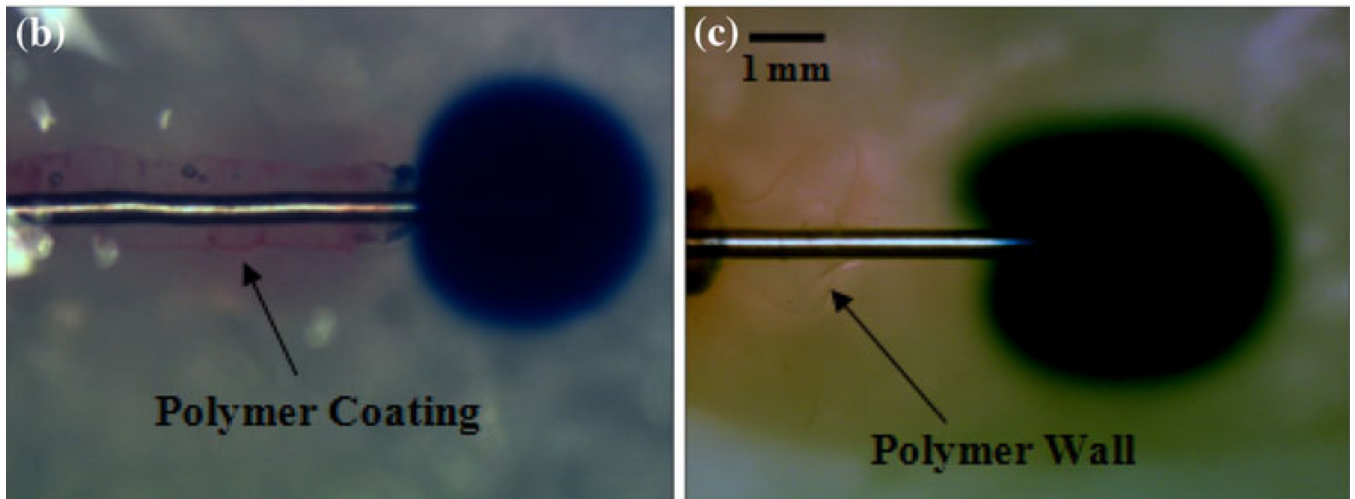
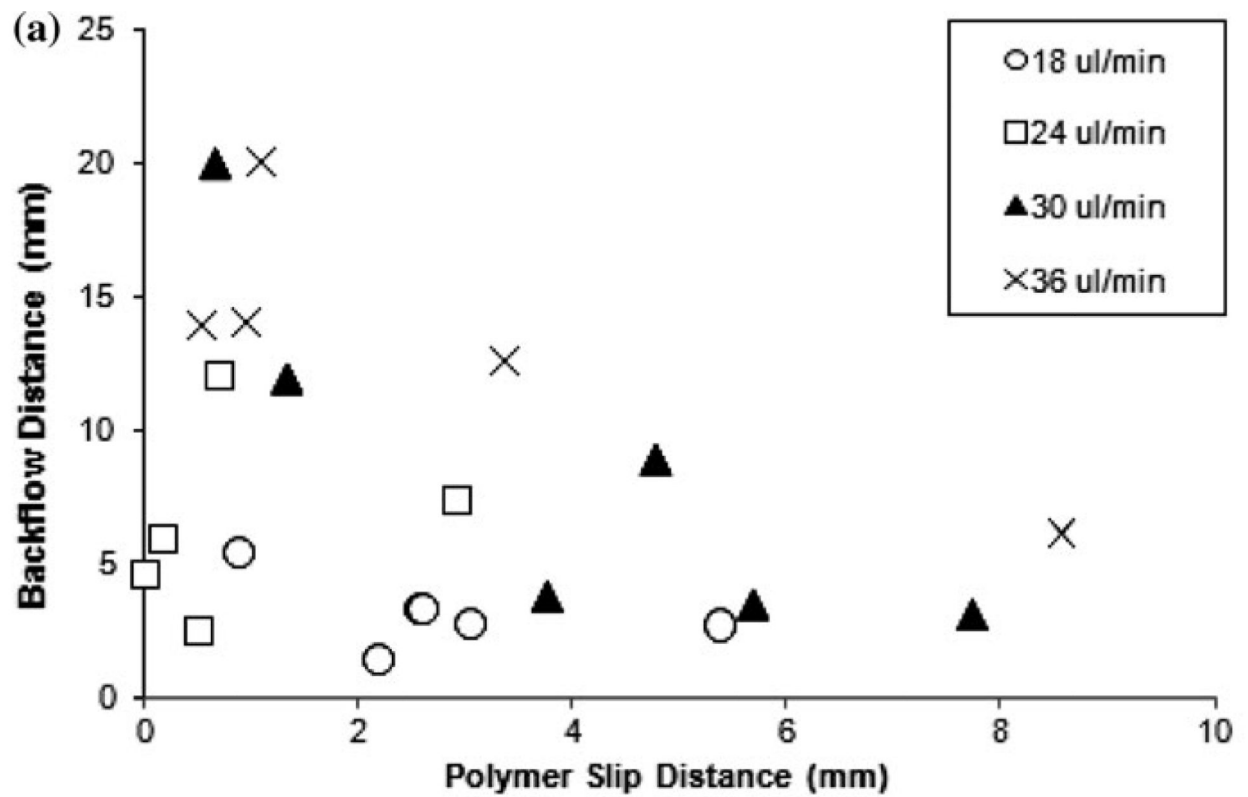


**Fig. 5.**  
**a** Backflow distances with increasing polymer slip distance. Slip distances were measured from the tip of the cannula to the edge of the polymer coating. **b** Backflow prevented upon contact with slipped polymer wall. **c** Backflow prevented before contacting polymer wall

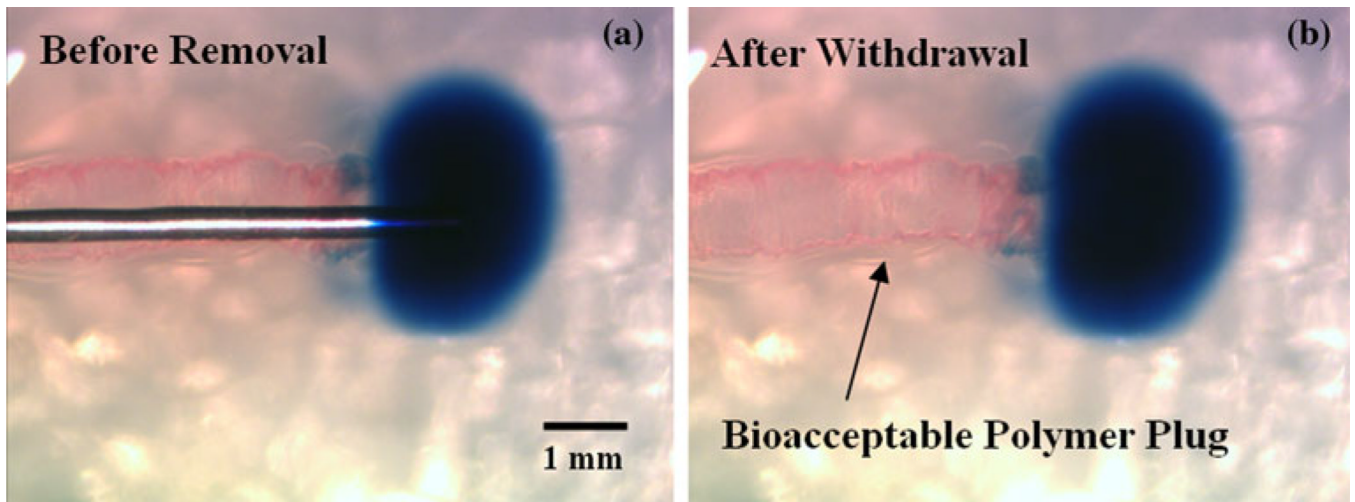


**Fig. 6.** **a** Polymer-coated cannula within hydrogel after tracer infusion (backflow is prevented upon contact with hydrated coating). **b** Polymer plug remained within cannula cavity after cannula removal. No further backflow of tracer was observed to occur within this implanted polymer seal

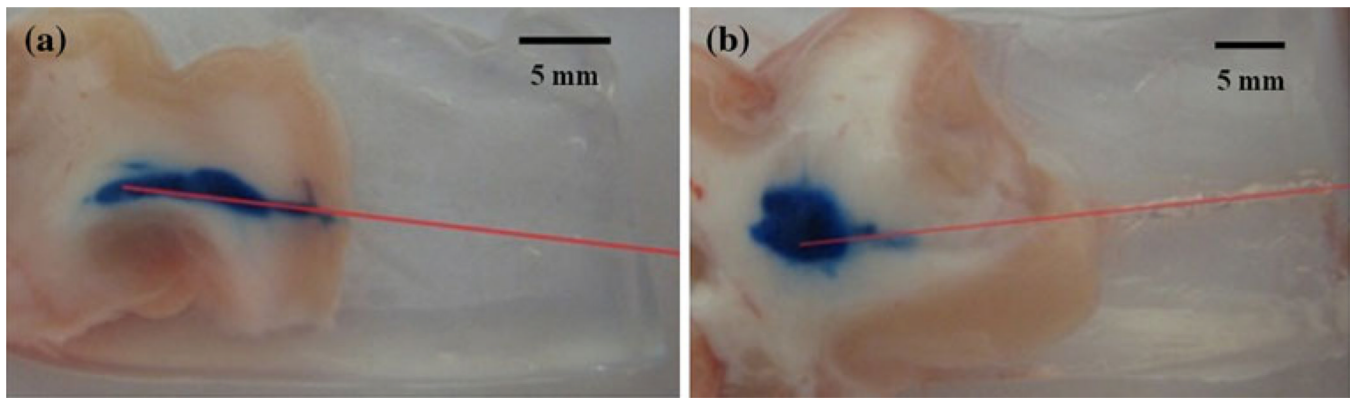


**Fig. 7.** Tracer infusions into white matter regions of porcine brain tissues. **a** Typical backflow observed when using uncoated needles. **b** With the dual-layered polymer coating applied to the cannulas, infusions showed significant reductions in backflow distances in the white matter. After withdrawal, the polymer coating was observed to stay in the cannula track. Estimated cannula tracks are drawn in *red* (Color figure online)

**Table 1**

Infusate backflow distances (mm) at varying infusion rates

Infusion trial	Infusion rates			
	0.3 $\mu\text{l min}^{-1}$	0.4 $\mu\text{l min}^{-1}$	0.5 $\mu\text{l min}^{-1}$	0.6 $\mu\text{l min}^{-1}$
1	3.2	1.9	20.0	6.1
2	5.4	7.3	3.8	20.0
3	2.7	2.4	3.5	13.9
4	3.3	5.9	11.9	14.0
5	1.4	4.6	3.1	12.5
6	2.7	12.1	8.9	1.6
Avg.	3.1	5.7	8.5	11.4
Std. dev.	1.3	3.7	6.7	6.5